

Muon $g - 2$ and CKM unitarity in extra lepton models

Motoi Endo^{a,b} and Satoshi Mishima^a

^aKEK Theory Center, IPNS, KEK,
Tsukuba, Ibaraki 305-0801, Japan

^bThe Graduate University of Advanced Studies (Sokendai),
Tsukuba, Ibaraki 305-0801, Japan

E-mail: motoi.endo@kek.jp, satoshi.mishima@kek.jp

ABSTRACT: We investigate the impact of extra leptons on observed tensions in the muon $g - 2$ and the first-row CKM unitarity. By introducing a new $SU(2)_L$ doublet lepton and a $SU(2)_L$ triplet lepton, we find that both of the tensions can be explained simultaneously under constraints from electroweak precision observables and Higgs-boson decays. Our model could be tested by measurements of $h \rightarrow \mu\mu$ at future collider experiments.

KEYWORDS: Beyond Standard Model, Effective Field Theories, Quark Masses and SM Parameters

ARXIV EPRINT: [2005.03933](https://arxiv.org/abs/2005.03933)

Contents

1	Introduction	1
2	Extra lepton model	3
3	Electroweak precision observables	6
4	Higgs decay	8
5	CKM unitarity	8
6	Muon $g - 2$	10
7	Result	12
8	Conclusions	17

1 Introduction

Flavor physics provides powerful probes for new physics (NP) beyond the Standard Model (SM). At present, some of flavor measurements show tensions with their SM predictions. In this paper, we investigate a tension in the anomalous magnetic moment of muon $a_\mu = (g_\mu - 2)/2$, so-called the muon $g - 2$, and that in the first-row unitarity of the Cabibbo-Kobayashi-Maskawa (CKM) matrix. They hint at NP that couples to muon.

The muon $g - 2$ exhibits a long-standing difference between the experimental measurement and the theory prediction in the SM. The latest value of the SM prediction is [1]¹

$$\Delta a_\mu = a_\mu^{\text{exp}} - a_\mu^{\text{SM}} = (27.9 \pm 7.6) \times 10^{-10}, \quad (1.1)$$

which corresponds to 3.7σ discrepancy. Here the experimental value is taken to be $a_\mu^{\text{exp}} = (11\,659\,208.9 \pm 5.4 \pm 3.3) \times 10^{-10}$, which is calculated from the result of the E821 experiment [5–7] with the latest value of the muon-to-proton magnetic ratio in the CODATA 2018 [8].² This discrepancy implies the potential existence of NP coupled to muon.³

The recent studies on the CKM matrix elements, V_{ud} and V_{us} , also show a tension with the CKM unitarity. The most precise determination of $|V_{ud}|$ comes at present from

¹A recent lattice study on the leading-order hadronic vacuum-polarization contribution shows no tension in the muon $g - 2$ [2]. The result is inconsistent by $> 3\sigma$ with those based on dispersive analyses for $e^+e^- \rightarrow$ hadron data [3, 4].

²Database developed by J. Baker, M. Douma and S. Kotochigova, <http://physics.nist.gov/constants>.

³The electron $g - 2$ with a precision measurement of the fine structure constant using caesium atoms also shows a discrepancy: $\Delta a_e = (-0.88 \pm 0.36) \times 10^{-12}$ [9]. We do not consider it in the current study.

the superallowed $0^+ \rightarrow 0^+$ nuclear β decays [10–12]. The extraction, however, suffers from theoretical uncertainty in the transition-independent part of hadronic contributions to electroweak (EW) radiative corrections [13]. Recent studies of them lead to

$$|V_{ud}| = \begin{cases} 0.97370 \pm 0.00014 & \text{(SGPR) [14],} \\ 0.97389 \pm 0.00018 & \text{(CMS) [15],} \\ 0.97365 \pm 0.00015 & \text{(SFGJ) [16],} \end{cases} \quad (1.2)$$

which are consistent with each other. On the other hand, $|V_{us}/V_{ud}|$ and $|V_{us}|$ are extracted from the leptonic-decay ratio $K_{\mu 2}/\pi_{\mu 2}$ and the semileptonic decays $K_{\ell 3}$ ($\ell = e, \mu$), respectively [17, 18]:

$$\left| \frac{V_{us}}{V_{ud}} \right| = 0.23129 \pm 0.00045, \quad |V_{us}| = 0.22326 \pm 0.00058. \quad (1.3)$$

The measured values of $|V_{ud}|$, $|V_{us}/V_{ud}|$ and $|V_{us}|$ violate the first-row CKM unitarity [19, 20]. Defining the amount of the violation as $|V_{ud}|^2 + |V_{us}|^2 + |V_{ub}|^2 = 1 + \Delta_{\text{CKM}}$ with $|V_{ub}| \approx 0.003683$ [21, 22], we have

$$\Delta_{\text{CKM}} = \begin{cases} -0.00118 \pm 0.00034, & \text{(SGPR, } K_{\mu 2}/\pi_{\mu 2}), \\ -0.00205 \pm 0.00038, & \text{(SGPR, } K_{\ell 3}), \\ -0.00079 \pm 0.00040, & \text{(CMS, } K_{\mu 2}/\pi_{\mu 2}), \\ -0.00168 \pm 0.00044, & \text{(CMS, } K_{\ell 3}), \\ -0.00128 \pm 0.00036, & \text{(SFGJ, } K_{\mu 2}/\pi_{\mu 2}), \\ -0.00215 \pm 0.00039, & \text{(SFGJ, } K_{\ell 3}), \end{cases} \quad (1.4)$$

which are away from zero at the 3.5σ , 5.4σ , 2.0σ , 3.8σ , 3.6σ and 5.5σ level, respectively.⁴ This violation may suggest a NP contribution to the W - μ - ν interaction [19, 23, 24].

Both of the above tensions imply NP that couples to muon. The effective field theory analysis tells us its energy scale. The effective Lagrangian for the muon $g-2$, $\mathcal{L}_{\text{eff}} = (1/\Lambda^2)(\bar{\ell}\sigma^{\mu\nu}\mu_R)\phi A_{\mu\nu} + \text{h.c.}$, where ϕ is the SM Higgs doublet, implies the NP scale $\Lambda \sim 300$ TeV to accommodate the tension in eq. (1.1). On the other hand, the NP contributions to the W - μ - ν interaction is described by $\mathcal{L}_{\text{eff}} = (1/\Lambda^2)(\phi^\dagger i \overleftrightarrow{D}_\mu^a \phi)(\bar{\ell}\gamma^\mu \sigma^a \ell)$, where σ^a are the Pauli matrices. The CKM tension in eq. (1.4) implies $\Lambda \lesssim 10$ TeV, which is one order of magnitude lower than the scale for the muon $g-2$. Namely, we expect that NP contributions to the CKM measurements are much larger than those to the muon $g-2$.

In this paper, we study extra lepton models as a candidate to solve the scale hierarchy in the NP contributions to the muon $g-2$ and the CKM measurements. The extra leptons can contribute to the latter at the tree level [25, 26], while effects on the former arise first at the one-loop level [26–37]. This explains naturally the hierarchy in the NP contributions.

⁴It is also noticed that the value of $|V_{us}|$ calculated by combining $|V_{us}/V_{ud}|$ from $K_{\mu 2}/\pi_{\mu 2}$ with $|V_{ud}|$ from the nuclear β decays is in tension with that from $K_{\ell 3}$ [17].

ℓ	μ_R	ϕ	$E_{L,R}$	$(\Delta_1)_{L,R}$	$(\Delta_3)_{L,R}$	$(\Sigma_1)_{L,R}$
$2_{-\frac{1}{2}}$	1_{-1}	$2_{\frac{1}{2}}$	1_{-1}	$2_{-\frac{1}{2}}$	$2_{-\frac{3}{2}}$	3_{-1}

Table 1. List of particles in the model. The quantum numbers represent $(\text{SU}(2)_L)_{\text{U}(1)_Y}$.

We investigate correlations between them under constraints from EW precision observables (EWPO) and the Higgs boson decay into a muon pair.⁵

This paper is organized as follows. In section 2 we present our extra lepton model and its matching to the SM effective field theory (SMEFT). In sections 3 and 4 we explain constraints from the EWPO and the Higgs boson decay, respectively. In sections 5 and 6 we discuss extra lepton contributions to the CKM measurements and the muon $g - 2$, respectively. In section 7 we present our numerical analysis. Finally our conclusions are drawn in section 8.

2 Extra lepton model

We introduce extra leptons which couple to the muons and have vectorlike masses.⁶ The particle contents are summarized in table 1.⁷ Here, $\ell = (\nu_L, \mu_L)^T$ is the SM $\text{SU}(2)_L$ doublet lepton in the second generation, and μ_R is the right-handed muon singlet. The Higgs doublet ϕ obtains a vacuum expectation value after the electroweak symmetry breaking (EWSB) as $\phi = [0, (v + h)/\sqrt{2}]^T$, where the Nambu-Goldstone bosons are ignored. The $\text{SU}(2)_L$ multiplets of the extra leptons are explicitly shown as

$$\Delta_1 = (\Delta_1^0, \Delta_1^-)^T, \quad \Delta_3 = (\Delta_3^-, \Delta_3^{--})^T, \quad (2.1)$$

$$\Sigma_1 = (\Sigma_1^1, \Sigma_1^2, \Sigma_1^3)^T = \left[\frac{\Sigma_1^0 + \Sigma_1^{--}}{\sqrt{2}}, \frac{i(\Sigma_1^0 - \Sigma_1^{--})}{\sqrt{2}}, \Sigma_1^- \right]^T. \quad (2.2)$$

In each field, the superscript 0, $-$, $--$ denotes the electric charge Q . Besides, $Q = 0$ for ν_L and -1 for $\mu_{L,R}$ and $E_{L,R}$. The gauge interactions are represented as

$$\begin{aligned} \mathcal{L}_{\text{int}} = & eQ\bar{f}\gamma^\mu f A_\mu \\ & + \frac{g}{c_W}\bar{f}\gamma^\mu [(T_L^3 - Qs_W^2)P_L + (T_R^3 - Qs_W^2)P_R]f Z_\mu \\ & + \frac{g}{\sqrt{2}}(\bar{\nu}\gamma^\mu\mu_L + \bar{\Delta}_i^0\gamma^\mu\Delta_i^- + \sqrt{2}\bar{\Sigma}_j^0\gamma^\mu\Sigma_j^- + \sqrt{2}\bar{\Sigma}_j^-\gamma^\mu\Sigma_j^{--})W_\mu^+ + \text{h.c.}, \end{aligned} \quad (2.3)$$

where A_μ , Z_μ and W_μ are the gauge bosons, and f represents a fermion in table 1 with $i = 1L, 1R, 3L, 3R$ and $j = 1L, 1R$ in the last line. Here and hereafter, $s_W = \sin\theta_W$ and

⁵Constraints from the lepton-flavor-universality violating ratios studied in refs. [23, 24] are weaker, and not considered in this study.

⁶If the extra leptons couple the electron or tau leptons simultaneously, lepton flavor violations are induced.

⁷In addition, a gauge singlet $N \sim 1_0$ and an $\text{SU}(2)_L$ adjoint lepton $\Sigma \sim 3_0$ are not included in the table because they are likely to generate too large neutrino masses by the seesaw mechanisms [38–42].

$c_W = \cos \theta_W$ with the Weinberg angle θ_W . The $SU(2)_L$ charge $T_{L,R}^3$ is shown as⁸

$$T_L^3 = \begin{cases} 1 & \text{for } \Sigma_{1L}^0, \\ 1/2 & \text{for } \nu_L, \Delta_{1L}^0, \Delta_{3L}^-, \\ 0 & \text{for } E_L, \Sigma_{1L}^-, \\ -1/2 & \text{for } \mu_L, \Delta_{1L}^-, \Delta_{3L}^-, \\ -1 & \text{for } \Sigma_{1L}^{--}, \end{cases} \quad T_R^3 = \begin{cases} 1 & \text{for } \Sigma_{1R}^0, \\ 1/2 & \text{for } \Delta_{1R}^0, \Delta_{3R}^-, \\ 0 & \text{for } \mu_R, E_R, \Sigma_{1R}^-, \\ -1/2 & \text{for } \Delta_{1R}^-, \Delta_{3R}^-, \\ -1 & \text{for } \Sigma_{1R}^{--}. \end{cases} \quad (2.4)$$

In general, the Yukawa interactions and vectorlike mass terms are given by

$$\begin{aligned} -\mathcal{L}_{\text{int}} = & y_\mu \bar{\ell} \phi \mu_R \\ & + \lambda_E \bar{E}_R \phi^\dagger \ell + \lambda_{\Delta_1} \bar{\Delta}_{1L} \phi \mu_R + \lambda_{\Delta_3} \bar{\Delta}_{3L} \tilde{\phi} \mu_R + \lambda_{\Sigma_1} \bar{\Sigma}_{1R}^a \phi^\dagger \sigma^a \ell \\ & + \lambda_{E\Delta_1} \bar{E}_L \phi^\dagger \Delta_{1R} + \lambda_{\Delta_1 E} \bar{\Delta}_{1L} \phi E_R \\ & + \lambda_{E\Delta_3} \bar{E}_L \tilde{\phi}^\dagger \Delta_{3R} + \lambda_{\Delta_3 E} \bar{\Delta}_{3L} \tilde{\phi} E_R \\ & + \lambda_{\Sigma_1 \Delta_1} \bar{\Sigma}_{1L}^a \phi^\dagger \sigma^a \Delta_{1R} + \lambda_{\Delta_1 \Sigma_1} \bar{\Delta}_{1L} \sigma^a \phi \Sigma_{1R}^a \\ & + \lambda_{\Sigma_1 \Delta_3} \bar{\Sigma}_{1L}^a \tilde{\phi}^\dagger \sigma^a \Delta_{3R} + \lambda_{\Delta_3 \Sigma_1} \bar{\Delta}_{3L} \sigma^a \tilde{\phi} \Sigma_{1R}^a \\ & + M_E \bar{E}_L E_R + M_{\Delta_1} \bar{\Delta}_{1L} \Delta_{1R} + M_{\Delta_3} \bar{\Delta}_{3L} \Delta_{3R} + M_{\Sigma_1} \bar{\Sigma}_{1L}^a \Sigma_{1R}^a + \text{h.c.}, \end{aligned} \quad (2.5)$$

where σ^a are the Pauli matrices and $\tilde{\phi} = i\sigma^2 \phi^*$. Here and hereafter, all the coupling constants are supposed to be real. Besides, the Yukawa couplings λ_E , λ_{Δ_1} , λ_{Δ_3} , and λ_{Σ_1} as well as the vectorlike masses M_i are chosen to be positive by rotating fields without loss of generality.

After the EWSB, the mass term of the singly-charged leptons is obtained as

$$-\mathcal{L}_m = \left[\bar{\mu}_L \quad \bar{E}_L \quad \bar{\Delta}_{1L}^- \quad \bar{\Delta}_{3L}^- \quad \bar{\Sigma}_{1L}^- \right] \mathcal{M}_- \begin{bmatrix} \mu_R \\ E_R \\ \Delta_{1R}^- \\ \Delta_{3R}^- \\ \Sigma_{1R}^- \end{bmatrix} + \text{h.c.}, \quad (2.6)$$

where the mass matrix \mathcal{M}_- is given in terms of the Yukawa matrix Y_- as

$$\mathcal{M}_- = \frac{v}{\sqrt{2}} Y_- + \text{diag}\left(0, M_E, M_{\Delta_1}, M_{\Delta_3}, M_{\Sigma_1}\right), \quad (2.7)$$

$$Y_- = \begin{bmatrix} y_\mu & \lambda_E & 0 & 0 & -\lambda_{\Sigma_1} \\ 0 & 0 & \lambda_{E\Delta_1} & \lambda_{E\Delta_3} & 0 \\ \lambda_{\Delta_1} & \lambda_{\Delta_1 E} & 0 & 0 & -\lambda_{\Delta_1 \Sigma_1} \\ \lambda_{\Delta_3} & \lambda_{\Delta_3 E} & 0 & 0 & \lambda_{\Delta_3 \Sigma_1} \\ 0 & 0 & -\lambda_{\Sigma_1 \Delta_1} & \lambda_{\Sigma_1 \Delta_3} & 0 \end{bmatrix}. \quad (2.8)$$

The matrix \mathcal{M}_- is diagonalized by a biunitary transformation:

$$U_L^{-\dagger} \mathcal{M}_- U_R^- = \text{diag}(m_{i^-}). \quad (2.9)$$

⁸It is noticed that the representation of Σ_1 in eq. (2.2) is not an eigenstate of the $SU(2)_L$ generator \hat{T}^3 . This is introduced to represent the Yukawa interactions in eq. (2.5).

Similarly, the mass terms of the neutral and doubly-charged leptons are written as

$$-\mathcal{L}_m = \left[\bar{\nu}_L \quad \bar{\Delta}_{1L}^0 \quad \bar{\Sigma}_{1L}^0 \right] \mathcal{M}_0 \begin{bmatrix} \nu_L^c \\ \Delta_{1R}^0 \\ \Sigma_{1R}^0 \end{bmatrix} + \left[\Delta_{3L}^{--} \quad \bar{\Sigma}_{1L}^{--} \right] \mathcal{M}_{--} \begin{bmatrix} \Delta_{3R}^{--} \\ \Sigma_{1R}^{--} \end{bmatrix} + \text{h.c.}, \quad (2.10)$$

$$\mathcal{M}_0 = \begin{bmatrix} 0 & 0 & v\lambda_{\Sigma_1} \\ 0 & M_{\Delta_1} & v\lambda_{\Delta_1\Sigma_1} \\ 0 & v\lambda_{\Sigma_1\Delta_1} & M_{\Sigma_1} \end{bmatrix}, \quad \mathcal{M}_{--} = \begin{bmatrix} M_{\Delta_3} & v\lambda_{\Delta_3\Sigma_1} \\ v\lambda_{\Sigma_1\Delta_3} & M_{\Sigma_1} \end{bmatrix}. \quad (2.11)$$

Note that the mass matrix \mathcal{M}_0 does not contribute to neutrino masses, i.e., avoiding too heavy neutrinos. These mass matrices are diagonalized as

$$U_L^{0\dagger} \mathcal{M}_0 U_R^0 = \text{diag}(m_{i^0}), \quad U_L^{--\dagger} \mathcal{M}_{--} U_R^{--} = \text{diag}(m_{i^{--}}). \quad (2.12)$$

After decoupling the extra leptons, whose masses are typically given by the vectorlike mass M_i , they contribute to low-energy observables through higher dimensional operators in the SMEFT. They are represented as

$$\mathcal{L}_{d=6} = \sum_j C_j \mathcal{O}_j, \quad (2.13)$$

where the dimension-six operators relevant for the current study are

$$\mathcal{O}_{e\phi} = (\phi^\dagger \phi)(\bar{\ell}\phi\mu_R), \quad (2.14)$$

$$\mathcal{O}_{\phi\ell}^{(1)} = (\phi^\dagger i \overleftrightarrow{D}_\mu \phi)(\bar{\ell}\gamma^\mu \ell), \quad (2.15)$$

$$\mathcal{O}_{\phi\ell}^{(3)} = (\phi^\dagger i \overleftrightarrow{D}_\mu^a \phi)(\bar{\ell}\gamma^\mu \sigma^a \ell), \quad (2.16)$$

$$\mathcal{O}_{\phi e} = (\phi^\dagger i \overleftrightarrow{D}_\mu \phi)(\bar{\mu}_R \gamma^\mu \mu_R). \quad (2.17)$$

Note that ℓ denotes the lepton doublet in the second generation. Here, the derivatives mean

$$\phi^\dagger \overleftrightarrow{D}_\mu \phi = \phi^\dagger (D_\mu \phi) - (D_\mu \phi)^\dagger \phi, \quad \phi^\dagger \overleftrightarrow{D}_\mu^a \phi = \phi^\dagger \sigma^a (D_\mu \phi) - (D_\mu \phi)^\dagger \sigma^a \phi. \quad (2.18)$$

The Wilson coefficients are obtained as [25, 43]

$$C_{e\phi} = y_\mu \left[\frac{\lambda_E^2}{2M_E^2} + \frac{\lambda_{\Delta_1}^2}{2M_{\Delta_1}^2} + \frac{\lambda_{\Delta_3}^2}{2M_{\Delta_3}^2} + \frac{\lambda_{\Sigma_1}^2}{2M_{\Sigma_1}^2} \right] - \frac{\lambda_E \lambda_{E\Delta_1} \lambda_{\Delta_1}}{M_E M_{\Delta_1}} - \frac{\lambda_E \lambda_{E\Delta_3} \lambda_{\Delta_3}}{M_E M_{\Delta_3}} - \frac{\lambda_{\Sigma_1} \lambda_{\Sigma_1\Delta_1} \lambda_{\Delta_1}}{M_{\Sigma_1} M_{\Delta_1}} + \frac{\lambda_{\Sigma_1} \lambda_{\Sigma_1\Delta_3} \lambda_{\Delta_3}}{M_{\Sigma_1} M_{\Delta_3}}, \quad (2.19)$$

$$C_{\phi\ell}^{(1)} = -\frac{\lambda_E^2}{4M_E^2} - \frac{3\lambda_{\Sigma_1}^2}{4M_{\Sigma_1}^2}, \quad (2.20)$$

$$C_{\phi\ell}^{(3)} = -\frac{\lambda_E^2}{4M_E^2} + \frac{\lambda_{\Sigma_1}^2}{4M_{\Sigma_1}^2}, \quad (2.21)$$

$$C_{\phi e} = \frac{\lambda_{\Delta_1}^2}{2M_{\Delta_1}^2} - \frac{\lambda_{\Delta_3}^2}{2M_{\Delta_3}^2}, \quad (2.22)$$

at the tree level. These coefficients are matched at the vectorlike mass scale. In the following analysis, we ignore renormalization group corrections below this scale for simplicity, which are induced by the $SU(2)_L$ and $U(1)_Y$ gauge interactions as well as the Yukawa couplings.

We define dimensionless coefficients as

$$\widehat{C}_i = v^2 C_i. \quad (2.23)$$

After the EWSB, the above operators modify the interactions of the Higgs, W and Z bosons from the SM predictions and affect low-energy observables. We will explain them in the following sections.

3 Electroweak precision observables

The Wilson coefficients $\widehat{C}_{e\phi}$, $\widehat{C}_{\phi\ell}^{(1)}$ and $\widehat{C}_{\phi\ell}^{(3)}$ are constrained strongly by the measurements of the EWPO, i.e., the Z and W boson observables (see refs. [44, 45] for flavor-dependent studies). The EWPO can be calculated with the SM input parameters: the Fermi constant G_F , the fine structure constant α , the strong coupling constant $\alpha_s(M_Z^2)$, the hadronic contribution $\Delta\alpha_{\text{had}}^{(5)}(M_Z^2)$ to the renormalization-group running of α , the Z -boson mass M_Z , the Higgs-boson mass m_h , the top-quark pole mass m_t , and other SM fermion masses. The measured values of the input parameters and the EWPO considered in this study are summarized in table 2.⁹ In our numerical analysis, the parameters G_F , α and the light fermion masses are fixed to be constants [47].

The operator $\mathcal{O}_{\phi\ell}^{(3)}$ alters the charged-current interactions of muon after the EWSB. Therefore the measured value of the Fermi constant G_F from the muon decay involves a contribution from $\mathcal{O}_{\phi\ell}^{(3)}$:

$$G_F = \frac{1}{\sqrt{2}v^2} \left(1 + \widehat{C}_{\phi\ell}^{(3)}\right) = \frac{1}{\sqrt{2}v^2} (1 + \delta_{G_F}), \quad (3.1)$$

where $\delta_{G_F} \equiv \widehat{C}_{\phi\ell}^{(3)}$. The modification of G_F affects the W -boson mass as

$$m_W = (m_W)_{\text{SM}} \left[1 - \frac{s_W^2}{2(c_W^2 - s_W^2)} \delta_{G_F}\right]. \quad (3.2)$$

Here and hereafter, a quantity with the subscript ‘‘SM’’ denotes the corresponding SM prediction calculated with the measured values of the input parameters G_F , α , M_Z , etc. The W -boson partial widths, which receive the corrections to M_W and those to the charged-current couplings, are given by

$$\Gamma(W^+ \rightarrow \mu^+ \nu_\mu) = \Gamma(W^+ \rightarrow \mu^+ \nu_\mu)_{\text{SM}} \left[1 - \frac{1 + c_W^2}{2(c_W^2 - s_W^2)} \delta_{G_F} + 2\widehat{C}_{\phi\ell}^{(3)}\right], \quad (3.3)$$

$$\Gamma(W^+ \rightarrow ij) = \Gamma(W^+ \rightarrow ij)_{\text{SM}} \left[1 - \frac{1 + c_W^2}{2(c_W^2 - s_W^2)} \delta_{G_F}\right], \quad (3.4)$$

where ij represents other final states including $e^+ \nu_e$, $\tau^+ \tau_\nu$, $d\bar{u}$ and $\bar{s}c$.

⁹The value of $\alpha_s(M_Z^2)$ is a lattice average calculated by the Flavour Lattice Averaging Group (FLAG) [46]. Also, the data of m_t is found in the review section on ‘‘Electroweak Model and Constraints on New Physics’’ of ref. [47].

	Measurement	Ref.		Measurement	Ref.
$\alpha_s(M_Z^2)$	0.1182 ± 0.0008	[46]	M_Z [GeV]	91.1876 ± 0.0021	[48]
$\Delta\alpha_{\text{had}}^{(5)}(M_Z^2)$	0.027609 ± 0.000112	[4]	Γ_Z [GeV]	2.4955 ± 0.0023	
m_t [GeV]	172.74 ± 0.46	[47]	σ_h^0 [nb]	41.4807 ± 0.0325	
m_h [GeV]	125.10 ± 0.14	[47]	R_e^0	20.8038 ± 0.0497	
M_W [GeV]	80.379 ± 0.012	[47]	R_μ^0	20.7842 ± 0.0335	
Γ_W [GeV]	2.085 ± 0.042	[47]	R_τ^0	20.7644 ± 0.0448	
$\mathcal{B}(W \rightarrow e\nu)$	0.1071 ± 0.0016	[49]	$A_{\text{FB}}^{0,e}$	0.0145 ± 0.0025	
$\mathcal{B}(W \rightarrow \mu\nu)$	0.1063 ± 0.0015		$A_{\text{FB}}^{0,\mu}$	0.0169 ± 0.0013	
$\mathcal{B}(W \rightarrow \tau\nu)$	0.1138 ± 0.002		$A_{\text{FB}}^{0,\tau}$	0.0188 ± 0.0017	
\mathcal{A}_e (SLD)	0.1516 ± 0.0021	[50]	R_b^0	0.21629 ± 0.00066	[50]
\mathcal{A}_μ (SLD)	0.142 ± 0.015		R_c^0	0.1721 ± 0.0030	
\mathcal{A}_τ (SLD)	0.136 ± 0.015		$A_{\text{FB}}^{0,b}$	0.0992 ± 0.0016	
\mathcal{A}_e (LEP)	0.1498 ± 0.0049	[50]	$A_{\text{FB}}^{0,c}$	0.0707 ± 0.0035	
\mathcal{A}_τ (LEP)	0.1439 ± 0.0043		\mathcal{A}_b	0.923 ± 0.020	
			\mathcal{A}_c	0.670 ± 0.027	

Table 2. Experimental measurement of the SM input parameters and EWPO.

The operator $\mathcal{O}_{\phi\ell}^{(3)}$ also affects the neutral-current interactions of left-handed muon and muon neutrino. In addition, the operators $\mathcal{O}_{\phi\ell}^{(1)}$ and $\mathcal{O}_{\phi e}$ modify the neutral-current interactions. Taking account of the NP contribution in G_F , the Z -boson couplings to the SM fermions f are modified as

$$\mathcal{L}_Z = \frac{g}{c_W} \bar{f} \gamma^\mu \left[(T_L'^3 - Qs_W^2 + \delta g_L) P_L + (T_R'^3 - Qs_W^2 + \delta g_R) P_R \right] f Z_\mu, \quad (3.5)$$

where the corrections δg_L and δg_R are given by

$$\delta g_L = \begin{cases} -\frac{1}{2} \left[T_L'^3 + \frac{Qs_W^2}{c_W^2 - s_W^2} \right] \delta_{G_F} - \frac{1}{2} \widehat{C}_{\phi\ell}^{(1)} + T_L'^3 \widehat{C}_{\phi\ell}^{(3)} & \text{for } f = \nu_L, \mu_L, \\ -\frac{1}{2} \left[T_L'^3 + \frac{Qs_W^2}{c_W^2 - s_W^2} \right] \delta_{G_F} & \text{otherwise,} \end{cases} \quad (3.6)$$

$$\delta g_R = \begin{cases} -\frac{Qs_W^2}{2(c_W^2 - s_W^2)} \delta_{G_F} - \frac{1}{2} \widehat{C}_{\phi e} & \text{for } f = \mu_R, \\ -\frac{Qs_W^2}{2(c_W^2 - s_W^2)} \delta_{G_F} & \text{otherwise.} \end{cases} \quad (3.7)$$

The Z -boson observables in table 2 are written in terms of the effective Zff couplings as shown, e.g., in ref. [51].

We perform a Bayesian fit of the Yukawa couplings λ_{Δ_1} , λ_{Δ_3} and λ_{Σ_1} to the experimental data of the EWPO, taking their correlations into account [48–50]. The Z -pole data at the LEP experiments have been updated recently in ref. [48], based on a sophisticated calculation of the Bhabha cross section, including beam-induced effects [52], for the measurement of the integrated luminosity. The fit is carried out with the `HEPfit` package [53], which is based on the Markov Chain Monte Carlo provided by the Bayesian Analysis Toolkit (BAT) [54]. The SM contributions to M_W and the Z -boson observables are calculated with the full two-loop EW corrections using the approximate formulae presented in refs. [55–57], while the W -boson widths are calculated at one-loop level [58, 59].

4 Higgs decay

The Higgs interactions are affected by the extra leptons through the SMEFT operators. The muon Yukawa interaction is affected by $\mathcal{O}_{e\phi}$ as

$$\mathcal{L}_{\text{Yukawa}} = -y_\mu \bar{\ell} \phi \mu_R + C_{e\phi} (\phi^\dagger \phi) (\bar{\ell} \phi \mu_R), \quad (4.1)$$

and thus, we obtain

$$y_\mu = \sqrt{2} \frac{m_\mu}{v} + \frac{1}{2} \widehat{C}_{e\phi}, = (y_\mu)_{\text{SM}} \left[1 - \frac{1}{2} \delta_{G_F} \right] + \frac{1}{2} \widehat{C}_{e\phi}, \quad (4.2)$$

after the EWSB. Then, the Yukawa interaction is rewritten as

$$\mathcal{L}_{\text{Yukawa}} = -m_\mu \bar{\mu}_L \mu_R - \frac{1}{\sqrt{2}} (y_\mu)_{\text{SM}} \left[1 - \frac{1}{2} \delta_{G_F} - \frac{1}{(y_\mu)_{\text{SM}}} \widehat{C}_{e\phi} \right] h \bar{\mu}_L \mu_R + \dots, \quad (4.3)$$

where $2h$ or $3h$ interactions are omitted. Consequently, the signal strength of the Higgs decay rate into muon pair is modified from the SM prediction as

$$\mu^{\mu\mu} \equiv \frac{\Gamma(h \rightarrow \mu\mu)}{\Gamma(h \rightarrow \mu\mu)_{\text{SM}}} = \left| 1 - \frac{1}{2} \delta_{G_F} - \frac{1}{(y_\mu)_{\text{SM}}} \widehat{C}_{e\phi} \right|^2. \quad (4.4)$$

Experimentally, only the upper limits are set at 95% CL as $\mu^{\mu\mu} < 2.1$ by ATLAS [60] and < 2.9 by CMS [61].¹⁰

5 CKM unitarity

In the current setup, although the unitarity of the CKM matrix is maintained, the extra leptons can affect extractions of the CKM elements from experimental data. In determining $|V_{ud}|$ from the superallowed $0^+ \rightarrow 0^+$ nuclear β decays, its transition rate is influenced by the extra leptons. For example, the decay rate of a β decay, $u \rightarrow d e^+ \nu$ is represented as

$$\Gamma_\beta \propto \frac{1}{v^4} |V_{ud}|^2 = 2G_F^2 |V_{ud}|^2 \left(1 + \widehat{C}_{\phi\ell}^{(3)} \right)^{-2}, \quad (5.1)$$

¹⁰To be exact, the upper limits are imposed on $\sigma(pp \rightarrow h) \times B(h \rightarrow \mu\mu) / \sigma(pp \rightarrow h)_{\text{SM}} \times B(h \rightarrow \mu\mu)_{\text{SM}}$. However, corrections of the extra leptons to the production cross section and the total decay rate of the Higgs boson are smaller by δ_{G_F} than the SM values, and thus, can be ignored safely.

via δ_{G_F} , where we used eq. (3.1) in the last equality. Thus, by taking the EW radiative corrections into account, the superallowed β decays satisfy the relation, (cf. ref. [12])

$$\begin{aligned} |V_{ud}|^2 &= \left(1 + \widehat{C}_{\phi\ell}^{(3)}\right)^2 \frac{K}{2\mathcal{F}t G_F^2 (1 + \Delta_R^V)} \\ &= \left(1 + \widehat{C}_{\phi\ell}^{(3)}\right)^2 \times \begin{cases} (0.97370 \pm 0.00014)^2 & \text{(SGPR)}, \\ (0.97389 \pm 0.00018)^2 & \text{(CMS)}, \\ (0.97365 \pm 0.00015)^2 & \text{(SFGJ)}, \end{cases} \end{aligned} \quad (5.2)$$

where $K = 8120.2776(9) \times 10^{-10} \text{ GeV}^{-4} \text{ s}$ and $\mathcal{F}t = 3072.07(63) \text{ s}$.¹¹ Also, the EW radiative corrections are given as

$$\Delta_R^V = \begin{cases} 0.02467 \pm 0.00022 & \text{(SGPR) [14]}, \\ 0.02426 \pm 0.00032 & \text{(CMS) [15]}, \\ 0.02477 \pm 0.00024 & \text{(SFGJ) [16]}. \end{cases} \quad (5.3)$$

The CKM element $|V_{us}|$ is determined by measuring the K meson decays. A ratio $|V_{us}/V_{ud}|$ is extracted from a ratio of the leptonic decay rates of the K and π mesons [18]:

$$\left| \frac{V_{us}}{V_{ud}} \right|^2 = \frac{\Gamma(K_{\mu 2}(\gamma))}{\Gamma(\pi_{\mu 2}(\gamma))} \frac{f_{\pi}^2}{f_K^2} \frac{m_{\pi\pm} (1 - m_{\mu}^2/m_{\pi\pm}^2)^2}{m_{K\pm} (1 - m_{\mu}^2/m_{K\pm}^2)^2} (1 - \delta) = (0.23129 \pm 0.00045)^2. \quad (5.4)$$

Here, f_K/f_{π} is a ratio of the K and π meson decay constants in the isospin limit, where the lattice results with $N_f = 2 + 1 + 1$ are adopted. The term δ takes account of EW radiative corrections and isospin-breaking effects. It is noticed that eq. (5.4) is independent of the extra lepton contributions because the decay rates depend on $\widehat{C}_{\phi\ell}^{(3)}$ as [23]

$$\Gamma(K_{\mu 2}(\gamma), \pi_{\mu 2}(\gamma)) \propto \frac{1}{v^4} |V_{us,ud}|^2 \left(1 + \widehat{C}_{\phi\ell}^{(3)}\right)^2 = 2G_F^2 |V_{us,ud}|^2, \quad (5.5)$$

where eq. (3.1) is employed.

The semileptonic K meson decay rates are also used to determine $|V_{us}|$. Their dependence on $\widehat{C}_{\phi\ell}^{(3)}$ are found as [23, 24]

$$\Gamma(K_{e3}) \propto \frac{1}{v^4} |V_{us}|^2 = 2G_F^2 |V_{us}|^2 \left(1 + \widehat{C}_{\phi\ell}^{(3)}\right)^{-2}, \quad (5.6)$$

$$\Gamma(K_{\mu 3}) \propto \frac{1}{v^4} |V_{us}|^2 \left(1 + \widehat{C}_{\phi\ell}^{(3)}\right)^2 = 2G_F^2 |V_{us}|^2. \quad (5.7)$$

Hence, $|V_{us}|$ satisfies the relation,

$$|V_{us}| = |V_{us}^{K_{e3}}| \left(1 + \widehat{C}_{\phi\ell}^{(3)}\right), \quad |V_{us}| = |V_{us}^{K_{\mu 3}}|, \quad (5.8)$$

where $|V_{us}^{K_{e3}, K_{\mu 3}}|$ are obtained by ignoring the extra lepton contributions, i.e., evaluated in the SM. They are estimated as

$$|V_{us}^{K_{e3}}| = 0.22320 \pm 0.00062, \quad |V_{us}^{K_{\mu 3}}| = 0.22345 \pm 0.00068, \quad (5.9)$$

¹¹There may be additional nuclear corrections to $\mathcal{F}t$, which can introduce extra uncertainties [62, 63].

where the input values are summarized in refs. [17, 64]. In particular, the form factor $f_+(0) = 0.9698(18)$ is obtained by lattice calculations with $N_f = 2 + 1 + 1$ [65, 66].¹²

The above CKM elements satisfy the first-row CKM unitarity,

$$|V_{ud}|^2 + |V_{us}|^2 + |V_{ub}|^2 = 1, \quad (5.10)$$

which gives a constraint on $\widehat{C}_{\phi\ell}^{(3)}$ as

$$\widehat{C}_{\phi\ell}^{(3)} = \begin{cases} (5.9 \pm 1.8) \times 10^{-4} & (\text{SGPR}, K_{\mu 2}/\pi_{\mu 2}), \\ (10.4 \pm 2.0) \times 10^{-4} & (\text{SGPR}, K_{e 3}), \\ (10.4 \pm 2.2) \times 10^{-4} & (\text{SGPR}, K_{\mu 3}), \\ (3.9 \pm 2.1) \times 10^{-4} & (\text{CMS}, K_{\mu 2}/\pi_{\mu 2}), \\ (8.5 \pm 2.3) \times 10^{-4} & (\text{CMS}, K_{e 3}), \\ (8.4 \pm 2.5) \times 10^{-4} & (\text{CMS}, K_{\mu 3}), \\ (6.4 \pm 1.8) \times 10^{-4} & (\text{SFGJ}, K_{\mu 2}/\pi_{\mu 2}), \\ (10.9 \pm 2.0) \times 10^{-4} & (\text{SFGJ}, K_{e 3}), \\ (10.9 \pm 2.2) \times 10^{-4} & (\text{SFGJ}, K_{\mu 3}), \end{cases} \quad (5.11)$$

where $|V_{ub}| = 0.003683(75)$ is used [21, 22].

In similar to the nuclear β decays, the decays of the π meson or the τ lepton are sensitive to the deviations of the W boson interactions from the SM predictions. In the current setup, the extra leptons couple only to the muons, and thus, violate the LFU between $\pi \rightarrow \mu\nu$ and $\pi \rightarrow e\nu$ or between $\tau \rightarrow \mu\nu\bar{\nu}$ and $\tau \rightarrow e\nu\bar{\nu}$. Although these decay modes give constraints on $\widehat{C}_{\phi\ell}^{(3)}$, the experimental uncertainties [47, 67–70] are still large, and the constraints are weaker.

6 Muon $g - 2$

The muon $g - 2$ receives corrections from the extra leptons which couple to the muons. In the mass eigenstate basis, the Higgs and gauge interactions are represented as

$$\begin{aligned} \mathcal{L}_{\text{int}} = & -\frac{1}{\sqrt{2}} g^{Hij} \bar{\psi}_{Li}^- \psi_{Rj}^- h + \frac{g}{c_W} g_{L,R}^{Zij} \bar{\psi}_i^- \gamma^\mu P_{L,R} \psi_j^- Z_\mu \\ & + \frac{g}{\sqrt{2}} g_{L,R}^{W^1ij} \bar{\psi}_i^0 \gamma^\mu P_{L,R} \psi_j^- W_\mu^+ + \frac{g}{\sqrt{2}} g_{L,R}^{W^2ij} \bar{\psi}_i^{--} \gamma^\mu P_{L,R} \psi_j^- W_\mu^- + \text{h.c.}, \end{aligned} \quad (6.1)$$

where the couplings are given by

$$g^{Hij} = \sum_{f,g} (U_L^-^\dagger)_{if} (Y_-)_{fg} (U_R^-)_{gj}, \quad (6.2)$$

$$g_{L,R}^{Zij} = \sum_f (U_{L,R}^-^\dagger)_{if} (T_{L,R}^3 - s_W^2 Q)_f (U_{L,R}^-)_{fj}, \quad (6.3)$$

¹²In ref. [17], the systematic uncertainty in the FNAL/MILC 18 result is taken to be 0.0011, but it has been updated to 0.0012 in the published version of the FNAL/MILC paper [66]. Accordingly, the uncertainty in $f_+(0)$ changes from 0.0017 to 0.0018.

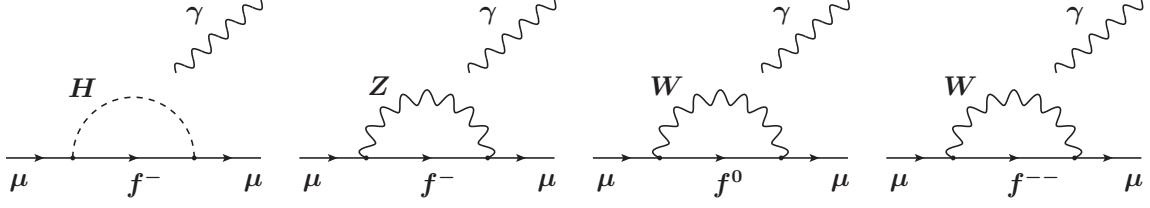


Figure 1. One-loop diagrams that contribute to the muon $g - 2$, where f^- , f^0 and f^{--} are extra leptons, and the photon attaches to charged particles.

$$g_{L,R}^{W^1ij} = \sum_f (U_{L,R}^{0\dagger})_{if} (U_{L,R}^-)_{fj} \times \begin{cases} 1 & \text{for } f = \ell, \Delta_{1L}, \Delta_{1R}, \\ \sqrt{2} & \text{for } f = \Sigma_{1L}, \Sigma_{1R}, \end{cases} \quad (6.4)$$

$$g_{L,R}^{W^2ij} = \sum_f (U_{L,R}'^{-\dagger})_{if} (U_{L,R}^-)_{fj} \times \begin{cases} 1 & \text{for } f = \Delta_{3L}, \Delta_{3R}, \\ \sqrt{2} & \text{for } f = \Sigma_{1L}, \Sigma_{1R}. \end{cases} \quad (6.5)$$

Here, the fields indexed by i, j are in the mass eigenstate basis, and f, g in g^{Hij} represent $\mu, E, \Delta_{1,3}^-$, and Σ_1 in the model basis. Also, f in g^{Zij} represent all the fields in table 1. Those in g^{W^1ij} run over the fields which include the charge-neutral component, $\ell, \Delta_{1L,1R}$ and Σ_1 . Similarly, f in g^{W^2ij} is effective for $\Delta_{3L,3R}$ and Σ_1 and vanishing for the others.

As shown in figure 1, the loop diagrams for the muon $g - 2$ are provided by exchanging the Higgs boson and singly-charged fermions for a_μ^H , the Z boson and singly-charged fermions for a_μ^Z , the W boson and neutrally-charged fermions for $a_\mu^{W^1}$, and the W boson with doubly-charged fermions for $a_\mu^{W^2}$. The formulae for those contributions are found in ref. [29] for the W and Z loop diagrams, while the reference [26] is used for the Higgs one. The results of the extra lepton contributions are summarized as

$$a_\mu^{\text{EL}} = a_\mu^H + a_\mu^Z + a_\mu^{W^1} + a_\mu^{W^2}, \quad (6.6)$$

where

$$a_\mu^H = \frac{m_\mu^2}{32\pi^2 m_H^2} \sum_{f^- \neq \mu} \left[\left[(g^{Hf^-1})^2 + (g^{H1f^-})^2 \right] F_{\text{FFS}}(x_{f-h}) + g^{Hf^-1} g^{H1f^-} \frac{m_{f^-}}{m_\mu} G_{\text{FFS}}(x_{f-h}) \right], \quad (6.7)$$

$$a_\mu^Z = \frac{m_\mu^2 G_F}{2\sqrt{2}\pi^2} \sum_{f^- \neq \mu} \left[\left[(g_L^{Zf^-1})^2 + (g_R^{Zf^-1})^2 \right] F_{\text{FFV}}(x_{f-Z}) + g_L^{Zf^-1} g_R^{Zf^-1} \frac{m_{f^-}}{m_\mu} G_{\text{FFV}}(x_{f-Z}) \right], \quad (6.8)$$

$$a_\mu^{W^1} = \frac{m_\mu^2 G_F}{4\sqrt{2}\pi^2} \times \sum_{f^0 \neq \nu} \left[\left[(g_L^{W^1f^0})^2 + (g_R^{W^1f^0})^2 \right] F_{\text{VVF}}(x_{f^0W}) + g_L^{W^1f^0} g_R^{W^1f^0} \frac{m_{f^0}}{m_\mu} G_{\text{VVF}}(x_{f^0W}) \right], \quad (6.9)$$

$$a_\mu^{W^2} = \frac{m_\mu^2 G_F}{4\sqrt{2}\pi^2} \sum_{f^{--}} \left[\left[(g_L^{W^2f^{--}})^2 + (g_R^{W^2f^{--}})^2 \right] \{ 2F_{\text{FFV}}(x_{f^{--}W}) - F_{\text{VVF}}(x_{f^{--}W}) \} \right. \\ \left. + g_L^{W^2f^{--}} g_R^{W^2f^{--}} \frac{m_{f^{--}}}{m_\mu} \{ 2G_{\text{FFV}}(x_{f^{--}W}) - G_{\text{VVF}}(x_{f^{--}W}) \} \right] \quad (6.10)$$

with $x_{ij} = m_i^2/m_j^2$. Here, the unitary matrices U_i in eqs. (6.2)–(6.5) are defined such that the mass eigenstates are ordered from lightest to heaviest, and thus, “1” in the indices of the coupling constants in eqs. (6.7)–(6.10) means the muon-like fermion in the mass eigenstate basis. The loop functions are defined as [29]

$$F_{\text{FFS}}(x) = \frac{1}{6(x-1)^4} [x^3 - 6x^2 + 3x + 2 + 6x \ln x], \quad (6.11)$$

$$G_{\text{FFS}}(x) = \frac{1}{(x-1)^3} [x^2 - 4x + 3 + 2 \ln x], \quad (6.12)$$

$$F_{\text{FFV}}(x) = \frac{1}{6(x-1)^4} [-5x^4 + 14x^3 - 39x^2 + 38x - 8 + 18x^2 \ln x], \quad (6.13)$$

$$G_{\text{FFV}}(x) = \frac{1}{(x-1)^3} [x^3 + 3x - 4 - 6x \ln x], \quad (6.14)$$

$$F_{\text{VVF}}(x) = \frac{1}{6(x-1)^4} [4x^4 - 49x^3 + 78x^2 - 43x + 10 + 18x^3 \ln x], \quad (6.15)$$

$$G_{\text{VVF}}(x) = \frac{1}{(x-1)^3} [-x^3 + 12x^2 - 15x + 4 - 6x^2 \ln x]. \quad (6.16)$$

All of the extra lepton contributions, eqs. (6.7)–(6.10), can be enhanced by λ_i/y_μ where $\lambda_i = \lambda_{E\Delta_1}, \lambda_{E\Delta_3}, \lambda_{\Sigma_1\Delta_1}$, and $\lambda_{\Sigma_1\Delta_3}$. In fact, any contribution to the muon $g-2$ involves a chirality flipping on the fermion line, and it is provided by these Yukawa couplings rather than the muon one. Consequently, Δa_μ is approximated as

$$a_\mu^{\text{EL}} = \sum_{i,j} \delta_{ij} \frac{v^2 \lambda_i \lambda_{ij} \lambda_j}{M_i M_j}, \quad (6.17)$$

for $M_E \sim M_{\Delta_1} \sim M_{\Delta_3} \sim M_{\sigma_1} \gg v$. The coefficients are estimated as $\delta_{ij} \sim -2 \times 10^{-6}$, -1×10^{-5} , -2×10^{-6} , and 2×10^{-6} for $(i,j) = (E, \Delta_1), (E, \Delta_3), (\Sigma_1, \Delta_1)$, and (Σ_1, Δ_3) . It is noticed that the sign of each contribution is determined by λ_{ij} . Besides, the Yukawa couplings $\lambda_{\Delta_1 E}, \lambda_{\Delta_3 E}, \lambda_{\Delta_1 \Sigma_1}, \lambda_{\Delta_3 \Sigma_1}$ do not affect the muon $g-2$ significantly.

The contributions that are not chirally enhanced are safely negligible in the limit of $M_i \gg v$. In particular, we do not include extra contributions from the SM loop diagrams, i.e., $f^-, f^0 \neq 1$ in eqs. (6.7)–(6.10). The SM Higgs, Z and W coupling constants are modified by the extra leptons via the unitary matrices U_i . Such deviations induce extra contributions by exchanging the SM particles in the loop diagrams. However, they are not chirally enhanced, and thus, ignored in the analysis.

7 Result

First of all, let us study the CKM unitarity in the extra lepton models. As we explained in section 5, $|V_{ud}|$ determined by the nuclear β decays and $|V_{us}|$ by K_{e3} are affected by $\widehat{C}_{\phi\ell}^{(3)}$, i.e., by E and Σ_1 among the extra leptons. The result is shown in figure 2, where $\widehat{C}_{\phi\ell}^{(3)}$ is plotted as functions of the Yukawa couplings λ_i . Here, the vectorlike masses are set to be $M_i = 2 \text{ TeV}$. The green band shows the 1σ region of $\widehat{C}_{\phi\ell}^{(3)}$ favored by the CKM unitarity, where the SFGJ result is adopted for $|V_{ud}|$ and the decay rates of $K_{\mu 2}, \pi_{\mu 2}$ are used for

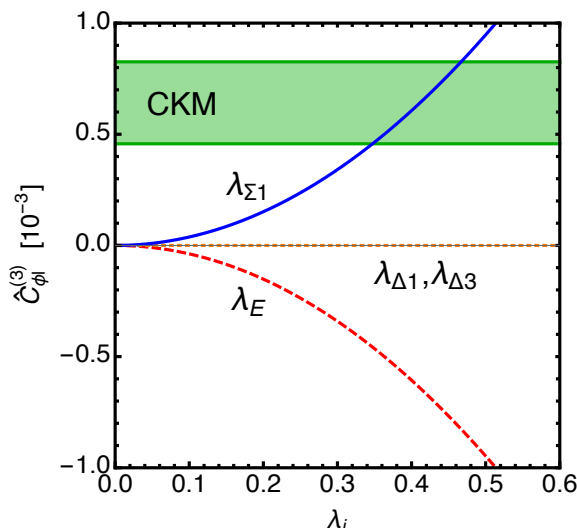


Figure 2. $\widehat{C}_{\phi\ell}^{(3)}$ in the extra lepton models with the vectorlike masses $M_i = 2 \text{ TeV}$. In the green band, $\widehat{C}_{\phi\ell}^{(3)}$ favored by the CKM unitarity is explained at the 1σ level, where the SFGJ value and the decay rates of $K_{\mu 2}, \pi_{\mu 2}$ are used.

$|V_{us}|$. It is found that only Σ_1 can relax the tension in the CKM unitarity. Depending on the evaluations of Δ_R^V and $|V_{us}|$, the CKM unitarity favors the regions,

$$\lambda_{\Sigma_1} = \begin{cases} 0.40 \pm 0.06 & (\text{SGPR}, K_{\mu 2}/\pi_{\mu 2}), \\ 0.52 \pm 0.05 & (\text{SGPR}, K_{e 3}), \\ 0.52_{-0.06}^{+0.05} & (\text{SGPR}, K_{\mu 3}), \\ 0.32_{-0.10}^{+0.08} & (\text{CMS}, K_{\mu 2}/\pi_{\mu 2}), \\ 0.47_{-0.07}^{+0.06} & (\text{CMS}, K_{e 3}), \\ 0.47_{-0.07}^{+0.06} & (\text{CMS}, K_{\mu 3}), \\ 0.41 \pm 0.06 & (\text{SFGJ}, K_{\mu 2}/\pi_{\mu 2}), \\ 0.54 \pm 0.05 & (\text{SFGJ}, K_{e 3}), \\ 0.54_{-0.06}^{+0.05} & (\text{SFGJ}, K_{\mu 3}), \end{cases} \quad (7.1)$$

at the 1σ level. This result is scaled by a ratio $\lambda_{\Sigma_1}/M_{\Sigma_1}$ for $M_{\Sigma_1} \neq 2 \text{ TeV}$ because $\widehat{C}_{\phi\ell}^{(3)}$ is proportional to the ratio squared. On the other hand, since the extra lepton E decreases $\widehat{C}_{\phi\ell}^{(3)}$, its contribution is favored to be decoupled by suppressing λ_E or assuming $M_E \gg v$. In the following analysis, we assume $\lambda_E = 0$.

Next, let us consider the tension in the muon $g - 2$. According to eq. (6.17), the contributions of Σ_1 can be chirally enhanced if it is accompanied by Δ_1 or Δ_3 . Once λ_{Δ_1} or λ_{Δ_3} is turned on, EWPO is also affected via $C_{\phi e}$ in similar to λ_{Σ_1} through $C_{\phi\ell}^{(1,3)}$. In figure 3, the muon $g - 2$ and EWPO as well as the CKM elements are evaluated as functions of the Yukawa couplings; in the top (bottom) plots, λ_{Σ_1} and λ_{Δ_1} (λ_{Δ_3}) are turned on, while $\lambda_{\Delta_3} = 0$ ($\lambda_{\Delta_1} = 0$) is assumed. Here, all the vectorlike masses are set to be $M_i = 2 \text{ TeV}$. In the left (right) plots, $|\lambda_{\Sigma_1 \Delta_{1,3}}| = 1$ (2) is chosen, and its sign is determined such that the

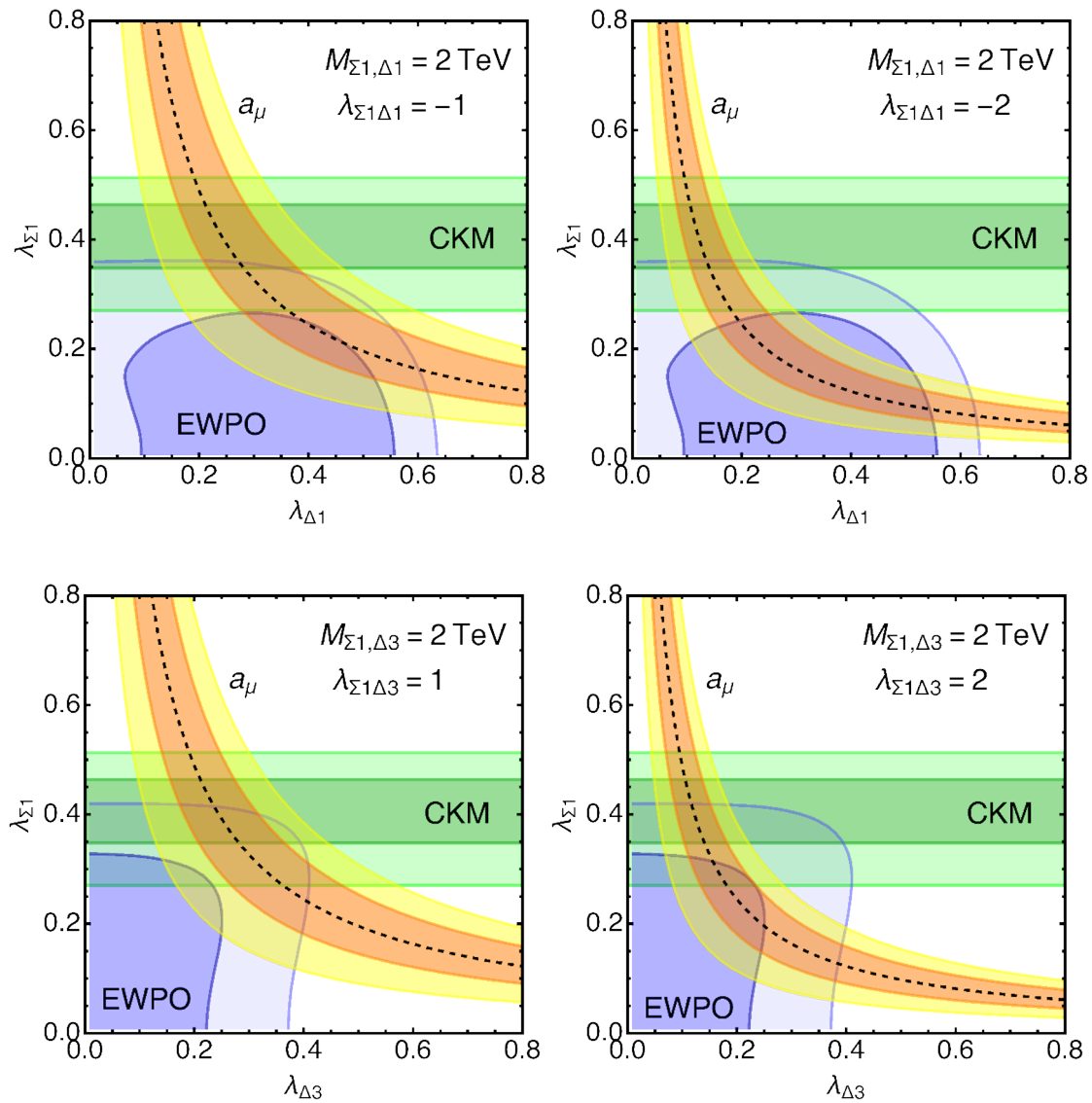


Figure 3. The CKM elements (green), a_μ (orange, yellow), EWPO (blue) and $\mu^{\mu\mu}$ are evaluated as functions of λ_{Σ_1} and $\lambda_{\Delta_{1,3}}$. The other Yukawa couplings which are not shown explicitly in each plot are set to be zero. For each observable, the current result is explained at the 1σ (2σ) level in the thick (thin) colored region, while the upper limit from the Higgs signal strength $\mu^{\mu\mu}$ is drawn by the black dashed line, where the left side is allowed at 95% CL by ATLAS. Here, the SFGJ value and the decay rates of $K_{\mu 2}, \pi_{\mu 2}$ are used to obtain the CKM regions.

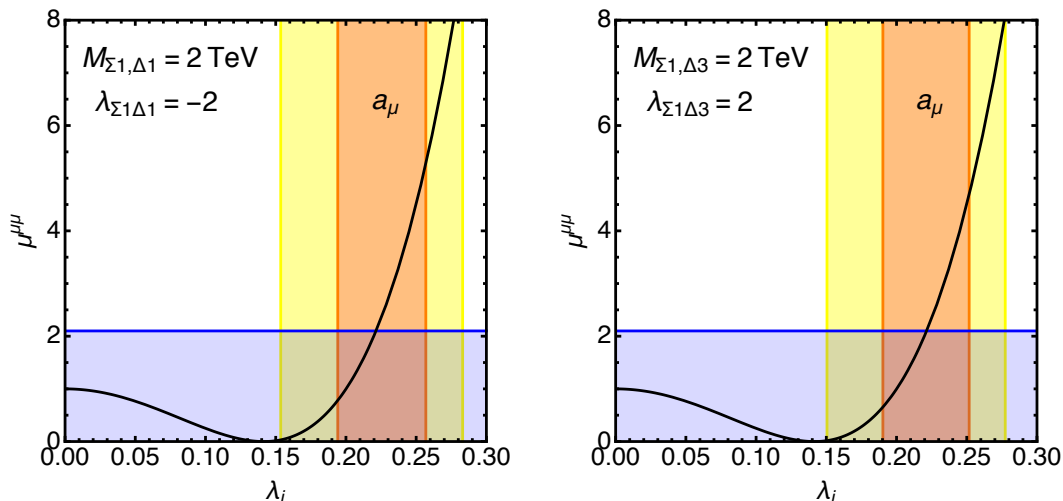


Figure 4. Signal strength of $h \rightarrow \mu\mu$ as a function of the Yukawa coupling λ_i . Here, $\lambda_i \equiv \lambda_{\Sigma_1} = \lambda_{\Delta_1}$ with $\lambda_{\Delta_3} = 0$ (left) and $\lambda_i \equiv \lambda_{\Sigma_1} = \lambda_{\Delta_3}$ with $\lambda_{\Delta_1} = 0$ (right). Also, $|\lambda_{\Sigma_1 \Delta_{1,3}}| = 2$ and $M_i = 2$ TeV. The blue region is allowed at 95% level by a search for $h \rightarrow \mu\mu$ at ATLAS. The discrepancy in the muon $g - 2$ is explained at the 1σ (2σ) level by the Yukawa couplings in the orange (yellow) region.

extra lepton contribution to the muon $g - 2$ becomes positive. Also, since all the observables are insensitive to $\lambda_{\Delta_{1,3}\Sigma_1}$, it is set to be zero here and hereafter. For each observable, the current data is explained at the 1σ (2σ) level in the thick (thin) colored region. Here, the SFGJ value is adopted for $|V_{ud}|$ and the decay rates of $K_{\mu 2}, \pi_{\mu 2}$ are used for $|V_{us}|$.

It is found that both of the tensions in the CKM unitarity and the muon $g - 2$ can be solved under the constraint from EWPO for $|\lambda_{\Sigma_1 \Delta_{1,3}}| = \mathcal{O}(1)$ at $M_i = 2$ TeV. Since the extra lepton contributions to the CKM elements and EWPO are proportional to powers of λ_i/M_i , the corresponding parameter regions are simply scaled from figure 3 as M_i is varied. On the other hand, since those to the muon $g - 2$ are scaled by $\lambda_{\Sigma_1} \lambda_{\Delta_{1,3}}/M_{\Sigma_1} M_{\Delta_{1,3}} \times \lambda_{\Sigma_1 \Delta_{1,3}}$, the parameter region favored by the muon $g - 2$ depends on $\lambda_{\Sigma_1 \Delta_{1,3}}$ in the figure.

The correction to the muon Yukawa interaction (4.2) is magnified if the extra lepton contribution to the muon $g - 2$ is enhanced. It is required to be as large as the SM value in the parameter region where the muon $g - 2$ is explained. Hence, tight parameter tunings between y_μ and the extra lepton contribution are not necessary to achieve the muon mass. However, such a contribution is limited by the Higgs decay rate into muon pair. In figure 4, the signal strength of the Higgs decay rate $\mu^{\mu\mu}$ is shown as a function of the Yukawa coupling $\lambda_i \equiv \lambda_{\Sigma_1} = \lambda_{\Delta_{1,3}}$. In the left plot, λ_{Δ_1} is turned on with $\lambda_{\Delta_3} = 0$, and $\Delta_1 \leftrightarrow \Delta_3$ in the right plot. Here, $|\lambda_{\Sigma_1 \Delta_{1,3}}| = 2$ and $M_i = 2$ TeV. The blue region is allowed at 95% level by ATLAS. On the other hand, the discrepancy in the muon $g - 2$ is explained at the 1σ (2σ) level by the Yukawa couplings in the orange (yellow) region. It is found that almost a half of the muon $g - 2$ parameter region is already excluded by $h \rightarrow \mu\mu$.

The constraint from $\mu^{\mu\mu}$ is also shown in figure 3. The left region of the black dashed line is allowed at 95% level. We conclude that both of the tensions in the CKM unitarity

and the muon $g - 2$ can be solved simultaneously under the constraints from $\mu^{\mu\mu}$ as well as the EWPO. Note that since the correction to the Yukawa interaction (2.19) is dominated by $\widehat{C}_{e\phi}$, its parameter dependence on λ_i and M_i is the same as that of the chirally-enhanced contribution to the muon $g - 2$ (6.17). Thus, the above conclusion is insensitive to the choice of $\lambda_{\Sigma_1\Delta_{1,3}}$ and M_i .

As seen from figure 4, the experimental uncertainty of $\mu^{\mu\mu}$ as well as that of the muon $g - 2$ is large. In particular, $\mu^{\mu\mu} = 1$, i.e., the SM value, is consistent with the current discrepancy of the muon $g - 2$. Thus, we cannot confirm/refute the extra lepton contribution yet, and it is significant to reduce both uncertainties. In future, the HL-LHC experiment may achieve $\delta\mu^{\mu\mu}/\mu^{\mu\mu} = 9\%$ at $\sqrt{s} = 14$ TeV with the integrated luminosity $\mathcal{L} = 6 \text{ ab}^{-1}$, and the uncertainty could be reduced by an order of magnitude compared to HL-LHC at FCC-ee/eh/hh [71]. Also, the experimental uncertainty of the muon $g - 2$ is planned to be reduced by a factor of 4 compared to the current value in the near future [72–75]. Therefore, we expect to check the extra lepton model by these measurements in future.

The extra leptons also contribute to the decay rate of the Higgs boson into two photons. The corrections are induced by δ_{G_F} and the extra lepton loops. They are estimated to be $\mathcal{O}(0.1)\%$ of the SM prediction, which is well within the current experimental uncertainty [76, 77]. In future, the experimental precision may become $\delta\mu^{\gamma\gamma}/\mu^{\gamma\gamma} = 3\%$ at HL-LHC with $\sqrt{s} = 14$ TeV and $\mathcal{L} = 6 \text{ ab}^{-1}$, and would be 0.6% at FCC-ee/eh/hh [71]. Thus, the extra lepton contribution to the two-photon channel could be probed in future.

In figure 3, the CKM elements are evaluated by adopting the SFGJ result and the decay rates of $K_{\mu 2}$ and $\pi_{\mu 2}$. If we use the CMS evaluation for Δ_R^V , the parameter overlapping with the EWPO region becomes better (see eq. (7.1) for a favored value of λ_{Σ_1}). On the other hand, larger λ_{Σ_1} is favored by V_{us} determined by $K_{\ell 3}$. The CKM region becomes consistent with the EWPO constraint at the 2σ level if the CMS evaluation is adopted, while it is not the case for SFGJ or SGPR. In any case, the tension between V_{ud} determined by the nuclear β decays and V_{us} by the K meson decay is relaxed by the extra lepton Σ_1 .¹³

Before closing this section, let us comment on the direct searches for the extra leptons. At collider experiments, they can be produced by exchanging the SM gauge bosons and decay predominantly into the SM bosons W, Z, h and the muonic leptons μ, ν . Such particles have signatures with multilepton final states. Although there are no experimental analyses based on the full dataset of LHC Run-II, the model may be excluded if the vectorlike masses are $M_i \sim 100$ GeV (cf. the CMS analysis [78] for the tauonic extra lepton search at $\sqrt{s} = 13$ TeV, and refs. [79–83] based on the LHC result at $\sqrt{s} = 8$ TeV). Thus, the setup with $M_i = 2$ TeV safely avoids the direct searches for the extra leptons at the LHC experiments. On the other hand, since future proton-proton colliders such as HL-LHC or higher energy colliders have potentials to probe those particles in multi-TeV scales [84], the extra leptons which solve the tensions in the CKM unitarity and the muon $g - 2$ could be discovered.¹⁴

¹³According to eq. (5.11), it is noticed that the discrepancy between V_{us} determined by $K_{\mu 2}, \pi_{\mu 2}$ and that by $K_{\ell 3}$ cannot be solved in the current framework.

¹⁴Triplet lepton searches are also studied for future electron-positron and electron-proton colliders [85].

8 Conclusions

Motivated by the tensions reported in the CKM unitarity and the muon $g - 2$, we studied the models of extra leptons which couple to the muon and have vectorlike masses. It was shown that the former tension is solved by introducing an $SU(2)_L$ triplet Σ_1 . In addition, the contribution to the muon $g - 2$ can be enhanced if it is accompanied by an $SU(2)_L$ doublet Δ_1 or Δ_3 . At the same time, the models are constrained by the EWPO and the Higgs boson decays. We found that both of the tensions can be solved simultaneously under these constraints. In particular, the Higgs decay rate into two muons is likely to be modified from the SM prediction significantly, and thus, could be useful to test the model at future experiments (see e.g., ref. [71]).

The above tensions are planned to be checked in future. Prospects for the test of the CKM unitarity and the LFU violations are discussed in ref. [24]. Also, the experimental value of the muon $g - 2$ will be updated in the near future [72–75]. Once the tensions would be confirmed, the extra lepton models can provide one of the attractive scenarios.

Acknowledgments

This work is supported in part by the Grant-in-Aid for Scientific Research B (No.16H03991 [ME]), Early-Career Scientists (No.16K17681 [ME]) and Scientific Research C (No.17K05429 [SM]).

Open Access. This article is distributed under the terms of the Creative Commons Attribution License ([CC-BY 4.0](https://creativecommons.org/licenses/by/4.0/)), which permits any use, distribution and reproduction in any medium, provided the original author(s) and source are credited.

References

- [1] T. Aoyama et al., *The anomalous magnetic moment of the muon in the Standard Model*, [arXiv:2006.04822](https://arxiv.org/abs/2006.04822) [[INSPIRE](#)].
- [2] S. Borsányi et al., *Leading-order hadronic vacuum polarization contribution to the muon magnetic moment from lattice QCD*, [arXiv:2002.12347](https://arxiv.org/abs/2002.12347) [[INSPIRE](#)].
- [3] M. Davier, A. Hoecker, B. Malaescu and Z. Zhang, *A new evaluation of the hadronic vacuum polarisation contributions to the muon anomalous magnetic moment and to $\alpha(m_Z^2)$* , *Eur. Phys. J. C* **80** (2020) 241 [*Erratum ibid.* **80** (2020) 410] [[arXiv:1908.00921](https://arxiv.org/abs/1908.00921)] [[INSPIRE](#)].
- [4] A. Keshavarzi, D. Nomura and T. Teubner, *$g - 2$ of charged leptons, $\alpha(M_Z^2)$, and the hyperfine splitting of muonium*, *Phys. Rev. D* **101** (2020) 014029 [[arXiv:1911.00367](https://arxiv.org/abs/1911.00367)] [[INSPIRE](#)].
- [5] MUON G-2 collaboration, *Measurement of the positive muon anomalous magnetic moment to 0.7 ppm*, *Phys. Rev. Lett.* **89** (2002) 101804 [*Erratum ibid.* **89** (2002) 129903] [[hep-ex/0208001](https://arxiv.org/abs/hep-ex/0208001)] [[INSPIRE](#)].
- [6] MUON G-2 collaboration, *Measurement of the negative muon anomalous magnetic moment to 0.7 ppm*, *Phys. Rev. Lett.* **92** (2004) 161802 [[hep-ex/0401008](https://arxiv.org/abs/hep-ex/0401008)] [[INSPIRE](#)].
- [7] MUON G-2 collaboration, *Final Report of the Muon E821 Anomalous Magnetic Moment Measurement at BNL*, *Phys. Rev. D* **73** (2006) 072003 [[hep-ex/0602035](https://arxiv.org/abs/hep-ex/0602035)] [[INSPIRE](#)].

- [8] E. Tiesinga, P.J. Mohr, D.B. Newell and B.N. Taylor, *The 2018 CODATA Recommended Values of the Fundamental Physical Constants*, Web Version 8.1, 2020.
- [9] R.H. Parker, C. Yu, W. Zhong, B. Estey and H. Müller, *Measurement of the fine-structure constant as a test of the Standard Model*, *Science* **360** (2018) 191 [[arXiv:1812.04130](#)] [[INSPIRE](#)].
- [10] J.C. Hardy and I.S. Towner, *Superaligned $0^+ \rightarrow 0^+$ nuclear β decays: 2014 critical survey, with precise results for V_{ud} and CKM unitarity*, *Phys. Rev. C* **91** (2015) 025501 [[arXiv:1411.5987](#)] [[INSPIRE](#)].
- [11] J. Hardy and I.S. Towner, *$|V_{ud}|$ from nuclear β decays*, *PoS CKM2016* (2016) 028 [[INSPIRE](#)].
- [12] J.C. Hardy and I.S. Towner, *Nuclear Beta Decays and CKM Unitarity*, in *13th Conference on the Intersections of Particle and Nuclear Physics*, (2018) [arXiv:1807.01146](#) [[INSPIRE](#)].
- [13] W.J. Marciano and A. Sirlin, *Improved calculation of electroweak radiative corrections and the value of $V(u,d)$* , *Phys. Rev. Lett.* **96** (2006) 032002 [[hep-ph/0510099](#)] [[INSPIRE](#)].
- [14] C.-Y. Seng, M. Gorchtein, H.H. Patel and M.J. Ramsey-Musolf, *Reduced Hadronic Uncertainty in the Determination of V_{ud}* , *Phys. Rev. Lett.* **121** (2018) 241804 [[arXiv:1807.10197](#)] [[INSPIRE](#)].
- [15] A. Czarnecki, W.J. Marciano and A. Sirlin, *Radiative Corrections to Neutron and Nuclear Beta Decays Revisited*, *Phys. Rev. D* **100** (2019) 073008 [[arXiv:1907.06737](#)] [[INSPIRE](#)].
- [16] C.-Y. Seng, X. Feng, M. Gorchtein and L.-C. Jin, *Joint lattice QCD-dispersion theory analysis confirms the quark-mixing top-row unitarity deficit*, *Phys. Rev. D* **101** (2020) 111301 [[arXiv:2003.11264](#)] [[INSPIRE](#)].
- [17] V. Cirigliano, M. Moulson and E. Passemar, *The status of V_{us}* , talk given at the workshop *Current and Future Status of First-Row CKM Unitarity*, UMass Amherst, May 2019, https://www.physics.umass.edu/acfi/sites/acfi/files/slides/moulson_amherst.pdf.
- [18] E. Passemar and M. Moulson, *Extraction of V_{us} from experimental measurements*, Talk given at the *International Conference on Kaon Physics 2019*, University of Perugia, September 2019, https://indico.cern.ch/event/769729/contributions/3512047/attachments/1905114/3146148/Kaon2019_MoulsonPassemarCorr.pdf.
- [19] B. Belfatto, R. Beradze and Z. Berezhiani, *The CKM unitarity problem: A trace of new physics at the TeV scale?*, *Eur. Phys. J. C* **80** (2020) 149 [[arXiv:1906.02714](#)] [[INSPIRE](#)].
- [20] Y. Grossman, E. Passemar and S. Schacht, *On the Statistical Treatment of the Cabibbo Angle Anomaly*, *JHEP* **07** (2020) 068 [[arXiv:1911.07821](#)] [[INSPIRE](#)].
- [21] CKMFITTER GROUP collaboration, *CP violation and the CKM matrix: Assessing the impact of the asymmetric B factories*, *Eur. Phys. J. C* **41** (2005) 1 [[hep-ph/0406184](#)] [[INSPIRE](#)].
- [22] CKMFITTER GROUP collaboration, http://ckmfitter.in2p3.fr/www/results/plots_summer19/num/ckmEval_results_summer19.html.
- [23] A.M. Coutinho, A. Crivellin and C.A. Manzari, *Global Fit to Modified Neutrino Couplings and the Cabibbo-Angle Anomaly*, [arXiv:1912.08823](#) [[INSPIRE](#)].
- [24] A. Crivellin and M. Hoferichter, *Beta decays as sensitive probes of lepton flavor universality*, [arXiv:2002.07184](#) [[INSPIRE](#)].
- [25] F. del Aguila, J. de Blas and M. Pérez-Victoria, *Effects of new leptons in Electroweak Precision Data*, *Phys. Rev. D* **78** (2008) 013010 [[arXiv:0803.4008](#)] [[INSPIRE](#)].

- [26] R. Dermisek and A. Raval, *Explanation of the Muon $g-2$ Anomaly with Vectorlike Leptons and its Implications for Higgs Decays*, *Phys. Rev. D* **88** (2013) 013017 [[arXiv:1305.3522](#)] [[INSPIRE](#)].
- [27] A. Czarnecki and W.J. Marciano, *The muon anomalous magnetic moment: A Harbinger for 'new physics'*, *Phys. Rev. D* **64** (2001) 013014 [[hep-ph/0102122](#)] [[INSPIRE](#)].
- [28] K. Kannike, M. Raidal, D.M. Straub and A. Strumia, *Anthropic solution to the magnetic muon anomaly: the charged see-saw*, *JHEP* **02** (2012) 106 [Erratum *ibid.* **10** (2012) 136] [[arXiv:1111.2551](#)] [[INSPIRE](#)].
- [29] A. Freitas, J. Lykken, S. Kell and S. Westhoff, *Testing the Muon $g-2$ Anomaly at the LHC*, *JHEP* **05** (2014) 145 [Erratum *ibid.* **09** (2014) 155] [[arXiv:1402.7065](#)] [[INSPIRE](#)].
- [30] E. Megias, M. Quirós and L. Salas, *$g_\mu - 2$ from Vector-Like Leptons in Warped Space*, *JHEP* **05** (2017) 016 [[arXiv:1701.05072](#)] [[INSPIRE](#)].
- [31] Z. Poh and S. Raby, *Vectorlike leptons: Muon $g-2$ anomaly, lepton flavor violation, Higgs boson decays, and lepton nonuniversality*, *Phys. Rev. D* **96** (2017) 015032 [[arXiv:1705.07007](#)] [[INSPIRE](#)].
- [32] K. Kowalska and E.M. Sessolo, *Expectations for the muon $g-2$ in simplified models with dark matter*, *JHEP* **09** (2017) 112 [[arXiv:1707.00753](#)] [[INSPIRE](#)].
- [33] S. Raby and A. Trautner, *Vectorlike chiral fourth family to explain muon anomalies*, *Phys. Rev. D* **97** (2018) 095006 [[arXiv:1712.09360](#)] [[INSPIRE](#)].
- [34] L. Calibbi, R. Ziegler and J. Zupan, *Minimal models for dark matter and the muon $g-2$ anomaly*, *JHEP* **07** (2018) 046 [[arXiv:1804.00009](#)] [[INSPIRE](#)].
- [35] A. Crivellin, M. Hoferichter and P. Schmidt-Wellenburg, *Combined explanations of $(g-2)_{\mu,e}$ and implications for a large muon EDM*, *Phys. Rev. D* **98** (2018) 113002 [[arXiv:1807.11484](#)] [[INSPIRE](#)].
- [36] J. Kawamura, S. Raby and A. Trautner, *Complete vectorlike fourth family and new $U(1)'$ for muon anomalies*, *Phys. Rev. D* **100** (2019) 055030 [[arXiv:1906.11297](#)] [[INSPIRE](#)].
- [37] J. Kawamura, S. Raby and A. Trautner, *Complete vectorlike fourth family with $U(1)'$: A global analysis*, *Phys. Rev. D* **101** (2020) 035026 [[arXiv:1911.11075](#)] [[INSPIRE](#)].
- [38] P. Minkowski, *$\mu \rightarrow e\gamma$ at a Rate of One Out of 10^9 Muon Decays?*, *Phys. Lett. B* **67** (1977) 421 [[INSPIRE](#)].
- [39] M. Gell-Mann, P. Ramond and R. Slansky, *Complex Spinors and Unified Theories*, [[arXiv:1306.4669](#)] [[INSPIRE](#)].
- [40] T. Yanagida, *Horizontal gauge symmetry and masses of neutrinos*, *Conf. Proc. C* **7902131** (1979) 95 [[INSPIRE](#)].
- [41] R.N. Mohapatra and G. Senjanović, *Neutrino Mass and Spontaneous Parity Nonconservation*, *Phys. Rev. Lett.* **44** (1980) 912 [[INSPIRE](#)].
- [42] R. Foot, H. Lew, X.G. He and G.C. Joshi, *Seesaw Neutrino Masses Induced by a Triplet of Leptons*, *Z. Phys. C* **44** (1989) 441 [[INSPIRE](#)].
- [43] J. de Blas, J.C. Criado, M. Pérez-Victoria and J. Santiago, *Effective description of general extensions of the Standard Model: the complete tree-level dictionary*, *JHEP* **03** (2018) 109 [[arXiv:1711.10391](#)] [[INSPIRE](#)].
- [44] A. Efrati, A. Falkowski and Y. Soreq, *Electroweak constraints on flavorful effective theories*, *JHEP* **07** (2015) 018 [[arXiv:1503.07872](#)] [[INSPIRE](#)].

- [45] A. Falkowski and D. Straub, *Flavourful SMEFT likelihood for Higgs and electroweak data*, *JHEP* **04** (2020) 066 [[arXiv:1911.07866](#)] [[INSPIRE](#)].
- [46] FLAVOUR LATTICE AVERAGING GROUP collaboration, *FLAG Review 2019: Flavour Lattice Averaging Group (FLAG)*, *Eur. Phys. J. C* **80** (2020) 113 [[arXiv:1902.08191](#)] [[INSPIRE](#)].
- [47] PARTICLE DATA GROUP collaboration, *Review of Particle Physics*, *Phys. Rev. D* **98** (2018) 030001 [[INSPIRE](#)].
- [48] P. Janot and S.a. Jadach, *Improved Bhabha cross section at LEP and the number of light neutrino species*, *Phys. Lett. B* **803** (2020) 135319 [[arXiv:1912.02067](#)] [[INSPIRE](#)].
- [49] ALEPH, DELPHI, L3, OPAL and LEP ELECTROWEAK collaborations, *Electroweak Measurements in Electron-Positron Collisions at W-Boson-Pair Energies at LEP*, *Phys. Rept.* **532** (2013) 119 [[arXiv:1302.3415](#)] [[INSPIRE](#)].
- [50] ALEPH, DELPHI, L3, OPAL, SLD, LEP ELECTROWEAK WORKING GROUP, SLD ELECTROWEAK GROUP and SLD HEAVY FLAVOUR GROUP collaborations, *Precision electroweak measurements on the Z resonance*, *Phys. Rept.* **427** (2006) 257 [[hep-ex/0509008](#)] [[INSPIRE](#)].
- [51] M. Ciuchini, E. Franco, S. Mishima and L. Silvestrini, *Electroweak Precision Observables, New Physics and the Nature of a 126 GeV Higgs Boson*, *JHEP* **08** (2013) 106 [[arXiv:1306.4644](#)] [[INSPIRE](#)].
- [52] G. Voutsinas, E. Perez, M. Dam and P. Janot, *Beam-beam effects on the luminosity measurement at LEP and the number of light neutrino species*, *Phys. Lett. B* **800** (2020) 135068 [[arXiv:1908.01704](#)] [[INSPIRE](#)].
- [53] J. De Blas et al., *HEPfit: a code for the combination of indirect and direct constraints on high energy physics models*, *Eur. Phys. J. C* **80** (2020) 456 [[arXiv:1910.14012](#)] [[INSPIRE](#)].
- [54] A. Caldwell, D. Kollar and K. Kroninger, *BAT: The Bayesian Analysis Toolkit*, *Comput. Phys. Commun.* **180** (2009) 2197 [[arXiv:0808.2552](#)] [[INSPIRE](#)].
- [55] M. Awramik, M. Czakon, A. Freitas and G. Weiglein, *Precise prediction for the W boson mass in the standard model*, *Phys. Rev. D* **69** (2004) 053006 [[hep-ph/0311148](#)] [[INSPIRE](#)].
- [56] M. Awramik, M. Czakon and A. Freitas, *Electroweak two-loop corrections to the effective weak mixing angle*, *JHEP* **11** (2006) 048 [[hep-ph/0608099](#)] [[INSPIRE](#)].
- [57] I. Dubovyk, A. Freitas, J. Gluza, T. Riemann and J. Usovitsch, *Electroweak pseudo-observables and Z-boson form factors at two-loop accuracy*, *JHEP* **08** (2019) 113 [[arXiv:1906.08815](#)] [[INSPIRE](#)].
- [58] D. Bardin, S. Riemann and T. Riemann, *Electroweak One Loop Corrections to the Decay of the Charged Vector Boson*, *Z. Phys. C* **32** (1986) 121 [[INSPIRE](#)].
- [59] A. Denner and T. Sack, *The W boson width*, *Z. Phys. C* **46** (1990) 653 [[INSPIRE](#)].
- [60] ATLAS collaboration, *A search for the rare decay of the Standard Model Higgs boson to dimuons in pp collisions at $\sqrt{s} = 13$ TeV with the ATLAS Detector*, *ATLAS-CONF-2018*, CERN, (2018).
- [61] CMS collaboration, *Search for the Higgs boson decaying to two muons in proton-proton collisions at $\sqrt{s} = 13$ TeV*, *Phys. Rev. Lett.* **122** (2019) 021801 [[arXiv:1807.06325](#)] [[INSPIRE](#)].
- [62] C.Y. Seng, M. Gorchtein and M.J. Ramsey-Musolf, *Dispersive evaluation of the inner radiative correction in neutron and nuclear β decay*, *Phys. Rev. D* **100** (2019) 013001 [[arXiv:1812.03352](#)] [[INSPIRE](#)].

- [63] M. Gorchtein, γW Box Inside Out: Nuclear Polarizabilities Distort the Beta Decay Spectrum, *Phys. Rev. Lett.* **123** (2019) 042503 [[arXiv:1812.04229](#)] [[INSPIRE](#)].
- [64] M. Moulson, *Experimental determination of V_{us} from kaon decays*, *PoS CKM2016* (2017) 033 [[arXiv:1704.04104](#)] [[INSPIRE](#)].
- [65] N. Carrasco, P. Lami, V. Lubicz, L. Riggio, S. Simula and C. Tarantino, $K \rightarrow \pi$ semileptonic form factors with $N_f = 2 + 1 + 1$ twisted mass fermions, *Phys. Rev. D* **93** (2016) 114512 [[arXiv:1602.04113](#)] [[INSPIRE](#)].
- [66] FERMILAB LATTICE and MILC collaborations, $|V_{us}|$ from $K_{\ell 3}$ decay and four-flavor lattice QCD, *Phys. Rev. D* **99** (2019) 114509 [[arXiv:1809.02827](#)] [[INSPIRE](#)].
- [67] PIENU collaboration, *Improved Measurement of the $\pi \rightarrow e\nu$ Branching Ratio*, *Phys. Rev. Lett.* **115** (2015) 071801 [[arXiv:1506.05845](#)] [[INSPIRE](#)].
- [68] G. Czappek et al., *Branching ratio for the rare pion decay into positron and neutrino*, *Phys. Rev. Lett.* **70** (1993) 17 [[INSPIRE](#)].
- [69] D.I. Britton et al., *Measurement of the $\pi^+ \rightarrow e^+$ neutrino branching ratio*, *Phys. Rev. Lett.* **68** (1992) 3000 [[INSPIRE](#)].
- [70] HFLAV collaboration, *Averages of b-hadron, c-hadron, and τ -lepton properties as of 2018*, [arXiv:1909.12524](#) [[INSPIRE](#)].
- [71] J. de Blas et al., *Higgs Boson Studies at Future Particle Colliders*, *JHEP* **01** (2020) 139 [[arXiv:1905.03764](#)] [[INSPIRE](#)].
- [72] MUON G-2 collaboration, *Muon (g-2) Technical Design Report*, [arXiv:1501.06858](#) [[INSPIRE](#)].
- [73] MUON G-2 collaboration, *The Muon g – 2 Experiment at Fermilab*, *EPJ Web Conf.* **212** (2019) 05003 [[arXiv:1905.00497](#)] [[INSPIRE](#)].
- [74] J-PARC G-2 collaboration, *Measurement of muon g-2 and EDM with an ultra-cold muon beam at J-PARC*, *Nucl. Phys. B Proc. Suppl.* **218** (2011) 242.
- [75] M. Abe et al., *A New Approach for Measuring the Muon Anomalous Magnetic Moment and Electric Dipole Moment*, *PTEP* **2019** (2019) 053C02 [[arXiv:1901.03047](#)] [[INSPIRE](#)].
- [76] CMS collaboration, *Combined measurements of Higgs boson couplings in proton-proton collisions at $\sqrt{s} = 13$ TeV*, *Eur. Phys. J. C* **79** (2019) 421 [[arXiv:1809.10733](#)] [[INSPIRE](#)].
- [77] ATLAS collaboration, *Combined measurements of Higgs boson production and decay using up to 80 fb^{-1} of proton-proton collision data at $\sqrt{s} = 13$ TeV collected with the ATLAS experiment*, *Phys. Rev. D* **101** (2020) 012002 [[arXiv:1909.02845](#)] [[INSPIRE](#)].
- [78] CMS collaboration, *Search for vector-like leptons in multilepton final states in proton-proton collisions at $\sqrt{s} = 13$ TeV*, *Phys. Rev. D* **100** (2019) 052003 [[arXiv:1905.10853](#)] [[INSPIRE](#)].
- [79] ATLAS collaboration, *Search for heavy lepton resonances decaying to a Z boson and a lepton in pp collisions at $\sqrt{s} = 8$ TeV with the ATLAS detector*, *JHEP* **09** (2015) 108 [[arXiv:1506.01291](#)] [[INSPIRE](#)].
- [80] A. Falkowski, D.M. Straub and A. Vicente, *Vector-like leptons: Higgs decays and collider phenomenology*, *JHEP* **05** (2014) 092 [[arXiv:1312.5329](#)] [[INSPIRE](#)].
- [81] R. Dermisek, J.P. Hall, E. Lunghi and S. Shin, *Limits on Vectorlike Leptons from Searches for Anomalous Production of Multi-Lepton Events*, *JHEP* **12** (2014) 013 [[arXiv:1408.3123](#)] [[INSPIRE](#)].

- [82] S.A.R. Ellis, R.M. Godbole, S. Gopalakrishna and J.D. Wells, *Survey of vector-like fermion extensions of the Standard Model and their phenomenological implications*, *JHEP* **09** (2014) 130 [[arXiv:1404.4398](#)] [[INSPIRE](#)].
- [83] N. Kumar and S.P. Martin, *Vectorlike Leptons at the Large Hadron Collider*, *Phys. Rev. D* **92** (2015) 115018 [[arXiv:1510.03456](#)] [[INSPIRE](#)].
- [84] P.N. Bhattiprolu and S.P. Martin, *Prospects for vectorlike leptons at future proton-proton colliders*, *Phys. Rev. D* **100** (2019) 015033 [[arXiv:1905.00498](#)] [[INSPIRE](#)].
- [85] A. Das, S. Mandal and T. Modak, *Testing triplet fermions at the electron-positron and electron-proton colliders using fat jet signatures*, [arXiv:2005.02267](#) [[INSPIRE](#)].